Available online at www.sciencedirect.com
SCIENCE DIRECT®

Journal of the European Ceramic Society 24 (2004) 3119–3128

www.elsevier.com/locate/jeurceramsoc

Magnesia–spinel microcomposites

Cemail Aksel*, Paul D. Warren[1], Frank L. Riley

Department of Materials, School of Process, Environmental and Materials Engineering, University of Leeds, Leeds LS2 9JT, UK

Received 10 July 2003; received in revised form 10 October 2003; accepted 16 October 2003

Abstract

This study used a model system of fully dense high purity MgO, incorporating micron size spinel prepared by hot-pressing. Spinel powder was obtained from two sources: (i) 0.5 μm alumina powder was incorporated into MgO by in situ reaction, and (ii) *preformed* 3 μm spinel powder. The thermal expansion mismatch between MgO and spinel particles led to the intergranular and intragranular crack development, with consequent loss of strength and Young's modulus. The extent of interlinking of the microcracking was determined to be a function of spinel particle size and volume fraction; the reasons for this were examined. The mechanical properties and R'''' parameter values of the microcomposites were reported. The thermal shock resistance of in situ formed 20% 0.5 μm and preformed 30% 3 μm spinel composites, in terms of the R'''' parameter, was predicted to be 4 to ~5 times better than that of pure MgO, respectively.

Keywords: Mechanical properties; $MgAl_2O_4$; MgO; Microcomposites; Thermal shock parameters

1. Introduction

1.1. Industrial application of MgO–spinel refractories

Magnesium aluminate spinel ($MgAl_2O_4$) is an important constituent of magnesia-based refractory materials. There are no natural deposits of spinel, which is therefore normally obtained by reaction of mixtures of MgO and Al_2O_3. Commercial sintered magnesia–spinel refractory materials are divided into three categories: magnesia rich, stoichiometric, and alumina rich.[1] Spinel is used as an additive in magnesia rich bricks, for example, for cement kiln linings. MgO rich magnesium aluminate spinel bricks are used in the cooling zone and in the upper side of the sintering zone of the cement kiln.[2,3] The stoichiometric type is similarly used in cement kiln linings, as well as an alumina-based castable in ladles, which can also have good resistance to corrosion and erosion.[4,5] The alumina rich type is being studied for use in alumina-based castables in order to improve resistance to slag penetration; 85–90 wt.% Al_2O_3 is suggested as the optimum.[6] A higher alumina content increases the spinel bonding and improves strength, and increased spinel bonding results in better spalling resistance.[6] Alumina rich magnesia spinel is also used in steel and aluminium production, petrochemical applications, and glass melting furnaces.[2]

A major reason for the use of spinel is its better resistance to thermal shock and alkali attack, which indicates two to three times longer service lives than other basic bricks such as conventional MgO-chrome.[7,8] Magnesia-chrome refractories were used for many years as high strength hot-face refractories in a range of systems, including rotary cement kilns and steel making vessels,[9] but there is risk of the contamination of ground water by hexavalent (VI) chromium ions leached from waste materials. $Cr^{(VI)}$ has been associated with allergic skin ulceration and carcinomas in humans.[9] Hexavalent chromium diffuses from the refractory into the cement clinker, and increases the risk of toxic reactions during processing of the cement.[7] Hence, a second significant reason for the escalating interest in spinel is to avoid the use of refractories containing chromium oxide. Magnesium aluminate spinel is therefore being used as an alternative second phase in magnesia–spinel and alumina-spinel refractories, allowing a wide range of compositions

* Corresponding author. Present address: Department of Materials Science and Engineering, Anadolu University, Iki Eylül Campus, Muttalip, 26470 Eskisehir, Turkey. Tel.: +90-222-3350580×6355; fax: +90-222-3239501.

E-mail address: caksel@anadolu.edu.tr (C. Aksel).

[1] Present address: Pilkington plc., Group Research, Technology Centre, Hall Lane, Lathom, L40 5UF Lancashire, UK.

0955-2219/$ - see front matter © 2003 Elsevier Ltd. All rights reserved.
doi:10.1016/j.jeurceramsoc.2003.10.036

and types for a large number of applications to be produced.[4,10,11] The main advantages of using magnesia–spinel bricks in cement kilns can also be summarised as follows:[11–17] (i) low thermal expansion coefficient of magnesia spinel bricks, (ii) high resistance to thermo-mechanical stress, (iii) chemically resistant to oil and ash deposits, (iv) high resistance to corrosion and changes in kiln atmosphere, (v) low content of secondary oxides, which results in minimal alteration in structure of the hot face in service, (vi) elimination of chromite, which makes the brick less susceptible to alkali attack in service, (vii) no toxic $Cr^{(VI)}$ ions leached from waste materials, and (viii) white cements can be made without discoloration problems caused by transition metal cations.

1.2. In situ and preformed spinel based refractories

In situ formed spinel-based refractories use the addition of an alumina source to form the spinel in situ by reaction with the magnesia matrix during sintering, where a strong bond between spinel grains and the magnesia matrix is formed. It has been reported[18] that initial spinel formation occurs around the periphery of the alumina particle and proceeds towards the particle centre. The strongly bonded peripheral spinel and a hollow core in these granules is claimed to give better fracture toughness.[18] The strength and high temperature fracture characteristics depend strongly on the level of impurities in the magnesia, and the type and distribution of secondary phases.[3,7,19] The complete conversion of the granular alumina is slow during manufacture of the spinel. Residual free alumina will continue to form spinel with associated expansion in service, at a rate that depends on temperature and time. A smaller alumina particle size gives faster spinel formation and improvement in densification behaviour, and the product magnesia–spinel composites has also better strength.[18,20]

The second type, *preformed*, which is technologically more advanced, is usually made by mixing 10–25% sintered or fused synthetic spinel with 75–90% sintered magnesia clinker.[21] Sintered magnesia–spinel clinker is formed by heating at ~1700 °C.[21] In contrast to the in situ reaction of alumina, which develops a strong spinel bond with magnesia, preformed spinel grain has little tendency to bond to the magnesia. It is stated[18] that preformed spinel in a magnesia matrix has a peripheral gap around the spinel grain, which appears to act as a crack initiator, and cracks propagate into the surrounding magnesia matrix. Cracks often emanate from sharp corners, and fracture is then arrested when the crack meets the peripheral gap of another spinel granule. It is claimed[18] that the mechanical properties of MgO–spinel refractories containing preformed spinel are more strongly influenced than the in situ formed spinel refractory by sintering temperature. The trend is that Young's modulus decreases significantly with increasing sintering temperature, which is converse to the trend declared by the in situ formed spinel. A possible explanation is that a greater degree of microcracking is being introduced when cooled from higher sintering temperature by virtue of the greater contraction rate of the MgO matrix relative to the spinel.

Spinel particles are added in various proportions to MgO in order to improve its thermal shock resistance. The reason for the improvement in thermal shock resistance is linked to the large difference in thermal expansion coefficient between magnesium oxide (mean value $\sim 13.5\times10^{-6}$ °C^{-1}) and spinel ($\sim 7.6\times10^{-6}$ °C^{-1}).[22,23] This difference leads to the development of large tensile hoop stresses, and eventually extensive microcracking, around spinel grains during cooling from fabrication temperatures in excess of 1600 °C.[24,25] At a certain temperature microcracks can only occur when the dispersed particle size is larger than a critical value. MgO–spinel composites with $\alpha_{spinel} < \alpha_{MgO}$ show low strengths because the radial cracks produced readily link together.[26–28] Thermal expansion mismatch between MgO and spinel therefore can lead to a reduction in strength, because of an increase in crack length and a decrease in Young's modulus.[29–35] The microcracks decrease the overall strength and stiffness, but they may also either be barriers to subsequent crack propagation in service, or allow stress relief during heating. Some transient healing of the cracks may occur on subsequent reheating during use of the refractory, caused by the relief of stress by microcrack propagation during loading.[1,12,13,36] The improved resistance to thermal shock in MgO–spinel composites can therefore be attributed to the microcrack networks developed around the spinel particles.[24,28,31–35] The ability of a material to resist crack propagation and further damage, and loss of strength on thermal shocking can be expressed by means of Hasselman's thermal shock damage resistance parameter, R''''.[37–39] The parameter R'''' can be applied to compare the degree of difficulty of generating crack length of materials with widely different values of γ_{WOF}, in brittle and ductile materials. It has already been reported that the predicted thermal shock parameters[25,26] and γ_{WOF}/γ_i ratios[26] are compared with the actual thermal shock behaviour, and R'''' parameter and γ_{WOF}/γ_i ratios are found to be good indicators for a quantitative evaluation of the retained strengths of MgO–spinel composites. It is also stated that resistance to thermal shock damage in terms of the effect of particle size distribution of spinel particles on the basis of thermal shock parameters can be more strongly favoured with materials containing significantly broader distribution of spinel particles, rather than narrow distributed spinel particles, for which a much larger volume% is required to achieve a similar improvement.[40]

The incorporation of spinel particles into magnesite refractories is known to increase thermal shock resistance. In this work, the effects of varying the amounts of spinel (5, 10, 20, 30 wt.%) and spinel particle sizes (0.5 and 3 μm) on the mechanical properties were investigated, where the attention was in general given to the different method of forming the spinel [as (i) in situ and (ii) preformed] rather than the different sizes of the spinel particles, which was already reported by the most recent researchers.[24–26,40] The strength, Young's modulus, critical defect size, MgO mean grain size, fracture surface energy, fracture toughness, work of fracture, and R'''' parameter values of the microcomposites are reported. The relationships between the mechanical properties and the changes in the microstructure and fracture surfaces of microcomposites were examined. In theory a fundamental requirements for better thermal shock damage resistance, in terms of the R'''' parameter, were predicted on the basis of the addition of in situ formed and *preformed* spinel particles.

2. Experimental

MgO of >98.0% purity ('light': GPR, BDH, Poole, UK), a nano-particle size powder, was calcined at 1300 °C for 2 h to produce a powder with a mean particle size of 0.5 μm. Spinel powder was obtained from two sources. Alumina powder (0.5 μm) with 99.8% purity (A16SG, Alcoa International Ltd., UK) was incorporated into MgO by in situ reaction. Alcoa MR66 preformed spinel powder (99.5% purity) was air classified to obtain more narrow distributions of median size 3 μm. The MgO–spinel composites, containing 0–30 wt.% spinel, could be obtained theoretically dense (~99%), by hot-pressing at 1720 °C and 20 MPa for 25 min. Bulk density and apparent porosity were measured using the standard water immersion method.[41] Mechanical measurements of all the spinel composites were carried out by three-point bend test, where support roller span was 20 mm, and the cross-head speed was 0.2 mm min^{-1}. Five specimens were normally tested to obtain a mean value, using a tensile testing machine (Mayes, SMT50). The standard equations for the strength (σ_f)[42] and Young's Modulus (E)[43] of a bar in three-point bend are:

$$\sigma_f = (3/2).(P.L)/(W.D^2) \quad (1)$$

$$E = L^3.m\ /(4.W.D^3) \quad (2)$$

where P: load at fracture, L: support span, W: specimen width, and D: specimen thickness, m: slope of the tangent of the initial straight-line portion of the load–deflection curve. Modulus values were calculated by drawing a tangent to the steepest initial straight-line portion of the load–deflection curve (the stiffness of the machine was also considered), using Eq. (2).[43] The standard equation[44–47] for the fracture toughness (K_{1c}) of a bar is:

$$K_{1c} = (3/2).(P.L.c^{1/2}).Y/(W.D^2) \quad (3)$$

$$Y = [A_0 + A_1(c/D) + A_2(c/D)^2 + A_3(c/D)^3 + A_4(c/D)^4] \quad (4)$$

where Y is a dimensionless parameter, which is dependent on the geometry of the loading and the crack configuration with $L/D \approx 8$, $A_0 = +1.96$, $A_1 = -2.75$, $A_2 = +13.66$, $A_3 = -23.98$, $A_4 = +25.22$,[47] and c is the notch depth. The fracture surface energy (γ_i), a measure of the resistance to initiation of crack propagation, was calculated from experimental K_{1c} (by SENB) and Young's modulus values using the standard relationship:

$$\gamma_i = K_{1c}^2\ /2E \quad (5)$$

Values for the work of fracture (γ_{WOF}) were calculated from load–deflection curves obtained from notched bars deformed in three-point bend, by measuring the area (U) under the load–deflection curve. γ_{WOF} is given by the following equation:[48,49]

$$\gamma_{WOF} = \{U/[2.W.(D-c)]\} \quad (6)$$

Thermal shock parameter R'''' was calculated from: $\{R'''' = (E.\gamma_{WOF})/[\sigma_f^2.(1-\nu)]\}$, which is the minimum in the extent of crack propagation on initiation of thermal stress fracture,[38,39] where ν is Poisson's ratio and γ_{WOF} is the work of fracture. The CamScan 4 SEM used in this study was equipped with an EDX system for element analysis. Secondary electron images (SEI) were used to examine the fracture surface, size, shape and texture of the particles; back scattered electron images (BEI), which provide atomic contrast, were used to indicate the presence and position of second phases in the polished surface of the multiphase materials. Grain sizes of polished and thermally etched (1500 °C, 10 min) surfaces were measured from photographs taken in the scanning electron microscope. Average grain size was determined from intercept measurements[50] on the observed plane, by using the standard Eq. (7):

$$\bar{D} = 1.56\bar{L} \quad (7)$$

where, $\bar{D}$ is the average grain size and $\bar{L}$ is the average intercept length, taken over a large number of grains and measured on the plane of polish. All the values calculated for pure MgO and spinel composites were the average value of ~100 measurements of three micrographs.

3. Results and discussion

Fig. 1 shows that the room temperature strength of the hot-pressed pure MgO was in good agreement with the literature values of ~225 and 230 MPa[29,51] for ~32 and 25 μm MgO grain sizes, respectively. The 0.5 μm in situ spinel composites prepared from A16 Al_2O_3 powder showed a ~20% decrease in strength for up to 10% addition, but further increases did not significantly affect strength (Fig. 1). Composites prepared from preformed 3 μm spinel powder showed a more marked decrease in strength with increasing amounts of spinel (Fig. 1). Although the overall pattern of behaviour was similar to that shown by the in situ spinel composites, there was a significant (>50%) decrease in strength of preformed composites at 20–30% addition probably because of more extensive microcracking in the composites (Fig. 2). The larger the spinel particles, the more the decline in strength (Fig. 1).

Young's moduli of composites decreased with additions of spinel, for each particle size (Fig. 3). Young's modulus of composites prepared using A16 Al_2O_3 approximately levelled out for up to 10% additions, but a more marked decrease (~45%) took place at 30% spinel loading (Fig. 3). The influence of the 3 μm spinel was greater, the larger the particle size. SEM observations in Fig. 2 showed that coarse particles were associated with longer crack formation, compared with finer particles (Fig. 4). The crack lengths also increased with increasing concentration of spinel. When the number of cracks and crack lengths increase, the actual area supporting the applied force decreases. Hence an increase in stress for a given load may produce more microcracks. The greater the extent of cracking, the greater the decrease in Young's modulus. The changes in Young's modulus can be explained in terms of crack development and interlinking, and these pre-existing cracks are assumed to be the result of thermal expansion mismatch between the MgO and spinel phase.[52] When the volume fraction of spinel increases, more microcracking occurs, and lower Young's modulus values are obtained.

SEM showed that preformed spinel grains in Fig. 2 were located at the MgO grain boundaries (intergranular) and within MgO grains (intragranular). In

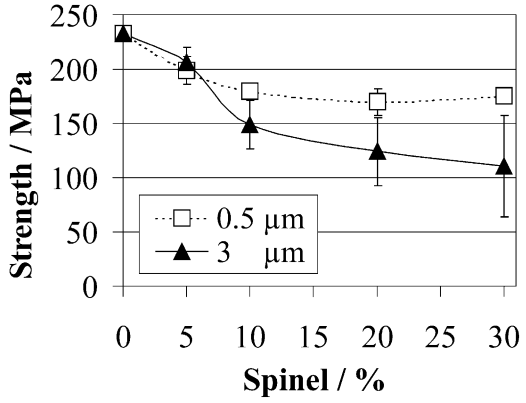

Fig. 1. Bend strength as a function of in situ formed (0.5 μm) and preformed (3 μm) spinel content.

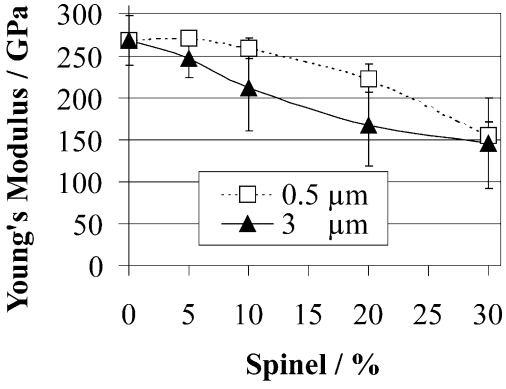

Fig. 3. Young's modulus as a function of in situ formed (0.5 μm) and preformed (3 μm) spinel content.

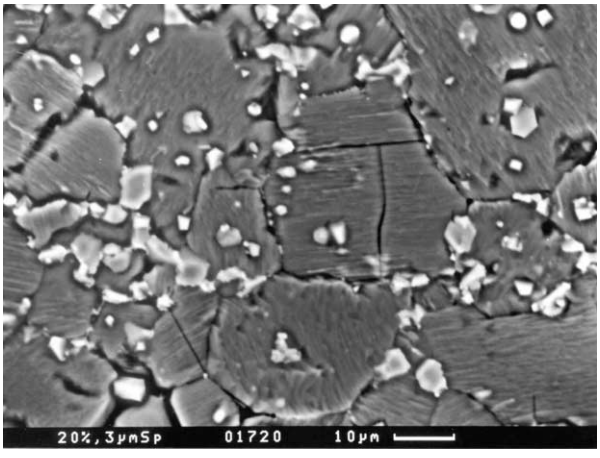

Fig. 2. SEM micrograph showing the microstructure of a 20% 3 μm preformed spinel composite.

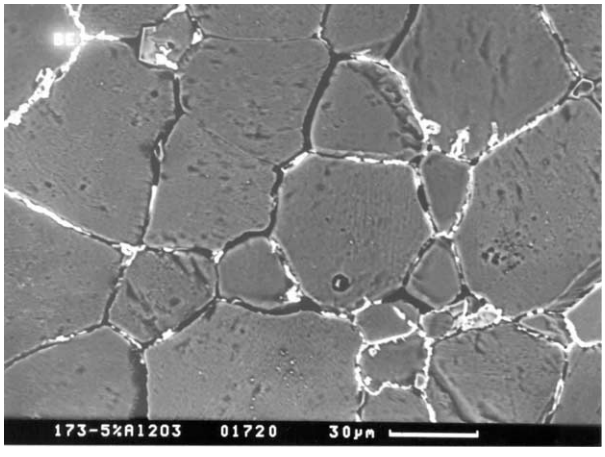

Fig. 4. SEM micrograph: MgO containing 0.5 μm—5% in situ spinel.

contrast, in situ formed spinel composites showed different microstructures, 0.5 μm particles are not uniformly distributed, but are mainly located at the MgO grain boundaries, and in close proximity to each other (Fig. 4). Combining the SENB fracture toughness values with those of strength allowed an estimate to be made of the critical defect size. Values are shown in Fig. 5. In general, intergranular and transgranular microcracks around the spinel particles formed: the amount of microcracking and the calculated crack defect size increased with spinel additions, and the finer the spinel particles the greater the extent of critical defect size of microcracking (Fig. 5).

The MgO–spinel composites thus have lower strengths and Young's moduli than the pure MgO materials. Both the strength and Young's modulus values of spinel composites in general decreased with increasing spinel content. Strength of preformed spinel composites appeared to be more sensitive to spinel content whereas the strength of the 0.5 μm spinel composites appeared to be relatively insensitive to composition. For the spinel composites, strength was more sensitive to spinel particle size, than was Young's modulus. Modulus appeared to be more sensitive to spinel content than to spinel particle size. For the in situ formed 0.5 μm spinel composites, there was not such a marked fall off in strength values with increasing spinel content, compared with Young's modulus.

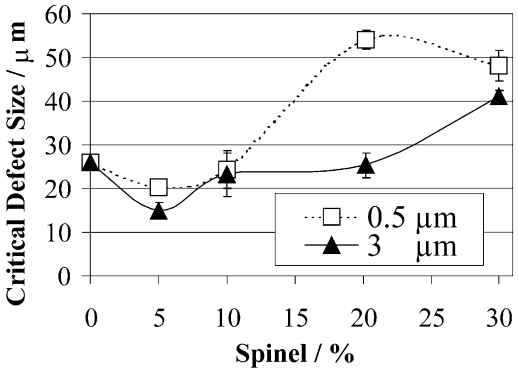

Fig. 5. Critical defect size as a function of in situ formed (0.5 μm) and preformed (3 μm) spinel content.

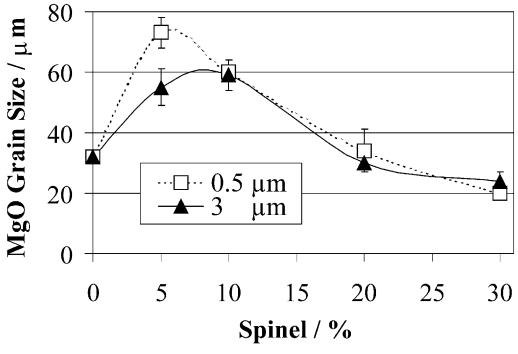

Fig. 6. MgO mean grain size, as a function of composite composition.

Fig. 6 shows that in all composites the mean grain size of MgO increased by a factor of ~2 to ~2.5, in the presence of 5 or 10% of spinel. However, further additions of spinel decreased the MgO grain size to approximately that of pure MgO, possibly because of a grain boundary pinning effect of the spinel particles located at the MgO grain boundaries (Figs. 4 and 7).

The fracture toughness (K_{1c}) of dense MgO ($\rho = 3.5$ Mg m^{-3}) measured using the single edge notched beam (SENB) technique was ~2.2 MPa m$^{1/2}$. This value is in good agreement with a literature value of ~2.05±0.05 MPa m$^{1/2}$ for materials with grain sizes ranging from 6 to 8 μm.[53] Composites prepared from 3 μm spinel showed a general marked decrease in toughness with increasing spinel content (Fig. 8). K_{1c} of 3 μm spinel composites decreased with up to 10% addition, and levelled out at a value of ~1.3 MPa m$^{1/2}$ with further additions. The marked decline in K_{1c} values of preformed spinel composites can (largely) be accounted for by the associated decrease in Young's modulus. K_{1c} for the in situ formed spinel composites initially decreased (e.g. for 5% 0.5 μm), but further spinel additions brought the values back to those of pure MgO (Fig. 8).

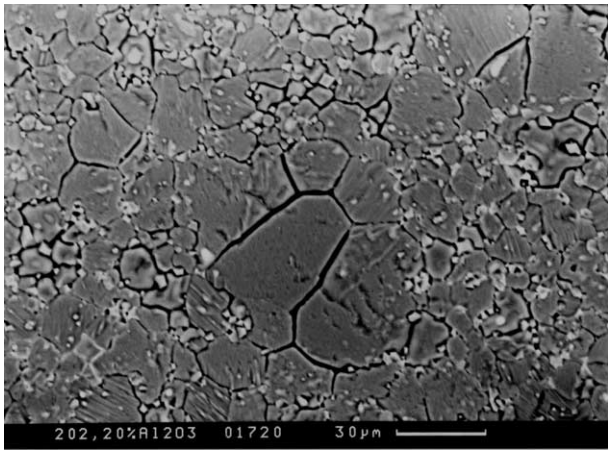

Fig. 7. SEM micrograph: MgO containing 0.5 μm—20% in situ spinel.

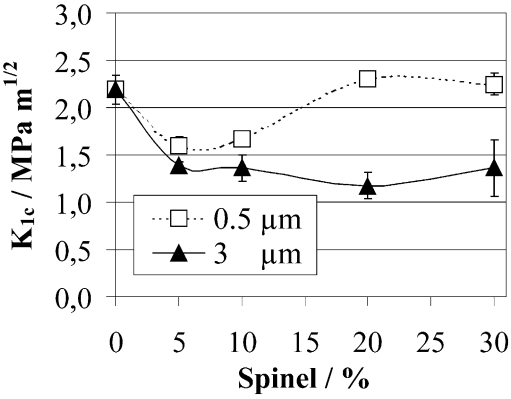

Fig. 8. Fracture toughness as a function of in situ formed (0.5 μm) and preformed (3 μm) spinel content.

This can be attributed to the special microstructure of this material (Figs. 4 and 7), with a different fracture path (Figs. 9–12), as compared with MgO and 3 μm preformed spinel composites. The significant change in fracture path from predominantly transgranular to mostly intergranular mode with a few but extensive amount of transgranular cracks is possibly the explanation for the marked increase in K_{1c} (e.g. back to the MgO value) at higher spinel contents.

The room temperature fracture surface energy of MgO obtained by using SENB (for a grain size ~100 μm) has been reported to be 14 J m^{-2},[54,55] and 15 J m^{-2}.[56] The fracture surface energy of dense spinel has been reported to be 4 ± 0.5 J m^{-2},[57] and 5 to 7 J m^{-2}.[58,59] These results are comparable to the values shown in Fig. 13. Fig. 13 shows that for the 3 μm spinel composites, γ_i values were lower than for pure MgO. In contrast, γ_i for the 0.5 μm spinel composites first decreased, and then sharply increased to give values almost twice those of pure MgO at 30% addition. This must again be attributed to the special microstructure of this material, and to the different fracture path. As would be expected, this pattern of behaviour in γ_i, calculated using experimental E and K_{1c} values, in general appeared to be similar to that of K_{1c} (Figs. 8 and 13).

At 5–10%, the 0.5 μm spinel composites had mostly transgranular fracture in the larger MgO grains (Fig. 10), and thus K_{1c} values associated with the amount of energy required to propagate cracking appeared to be smaller (Figs. 8 and 13), because of possible action of spinel particles located at the grain boundaries (Fig. 4). In contrast, the increase in K_{1c} and thereby γ_i with further additions of 0.5 μm spinel composites might be because of the mostly intergranular, with some transgranular, fracture in the smaller MgO grains (Fig. 11). Moreover, higher loading of 0.5 μm spinel particles (20–30%) gave different microstructures (Figs. 4 and 7), showing the location of spinel particles both within the grains and along the grain boundaries (Fig. 7), where MgO grain size was also very low (~32 μm). It is therefore possible that the marked increase at 20–30% in K_{1c} and γ_i was because intergranular cracks in the smaller MgO grain matrix require much more energy for fracture than those of lower additions.

Figs. 8 and 13 show that the decreasing trend in K_{1c} and γ_i, with further additions, is in general most marked for the coarser spinel particles in which the concentration of interconnected cracks appears to be the greatest. The energy required to propagate a crack decreases as the concentration of pre-existing connected cracks increases, which it does as the spinel concentration increases (Fig. 2). At 5% with additions of preformed spinel, the amount of cracking and crack size was limited; it appears that pre-existing connected cracks could not propagate easily. Therefore more

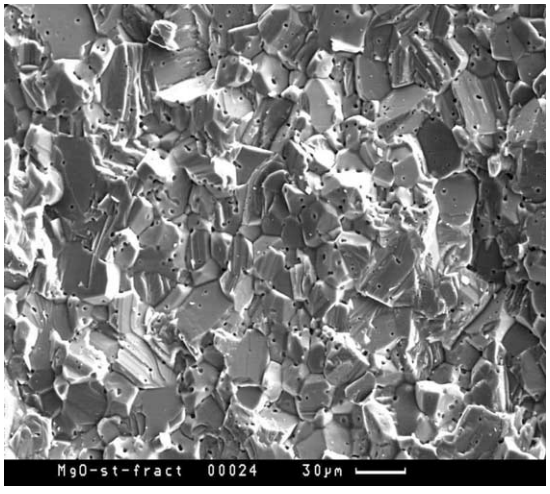

Fig. 9. Fracture surface of dense MgO.

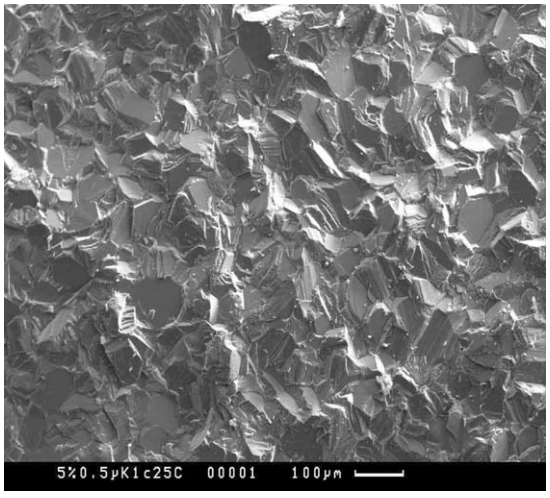

Fig. 10. Fracture surface of composite containing 5% 0.5 μm in situ formed spinel.

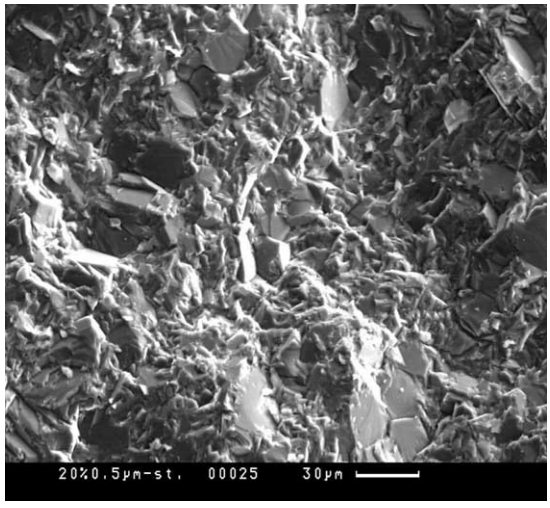

Fig. 11. Fracture surface of composite containing 20% 0.5 μm in situ formed spinel.

energy was required to connect the cracks for propagation with further spinel additions.

The measured work of fracture (obtained from the areas under the stress-strain curve) in this work is comparable with that of 35 J m^{-2} (Ref. 60) for polycrystalline fully dense MgO (3.56 Mg m^{-3}) of ~100 μm average grain size (Fig. 14). The work of fracture value of in situ formed 0.5 μm spinel increased only slightly with up to 10% additions, but at 20% it increased by a factor of 2.5 (Fig. 14). At composites containing ⩾20% spinel additions, primarily intergranular fracture occurred through the smaller MgO grains, and it appears to require more energy to propagate a crack completely through the specimen (Fig. 11). In 3 μm spinel composites, there was a general but less marked increase in γ_{WOF}, by a factor of ~2, at 30% additions (Fig. 14). It seems that the effect of spinel content is more important than particle size, within the larger scatter data.

Fracture surfaces of MgO showed that there was some intergranular fracture (along the grain boundaries), but the fracture was mostly transgranular (through the grains) with clear grain cleavage (Fig. 9). Composites containing 5–10% 0.5 μm in situ formed spinel showed mostly transgranular, with some intergranular, fracture (Fig. 10). In contrast, with 20–30% of 0.5 μm spinel the proportion of intergranular fracture increased markedly, with a few but significant amount of transgranular cracks (Fig. 11). It is possible that mostly intergranular fracture along the smaller MgO grains, at higher spinel loading, requires much more energy for fracture than that for lower spinel loading, and this causes an increase in γ_i, and gives much higher γ_{WOF} values (Figs. 13 and 14). Three micrometre spinel composites with low spinel content showed a large proportion of transgranular cracks in the fracture surfaces, like MgO. However, intergranular fracture was predominantly observed with increasing spinel content (Fig. 12). This change in fracture path from predominantly transgranular to more intergranular fracture, with further spinel additions, is thought to be the main reason for the increase in γ_{WOF} energy required to propagate a crack completely through a specimen (Fig. 14).

There was an interest to investigate how strength and Young's modulus varied for each composition, due to the importance of the strength and Young's modulus ratios for calculation of thermal shock parameters. The R'''' parameter gives information about the ability of the material to resist crack propagation and further damage and loss of strength on thermal shocking, with different values of γ_{WOF}, and high values indicate an improvement in thermal shock resistance. Fig. 15 shows that R'''' increased with the additions of in situ formed 20% 0.5 μm and preformed 30% 3 μm spinel to a maximum, with an improvement by a factor of ⩾4 and ~5, respectively, as compared with pure MgO. Young's modulus for further additions was more strongly influenced by composition than was strength (Figs. 1 and 3). These variations in R'''' parameter are probably because for up to 10% spinel addition strength was more sensitive to

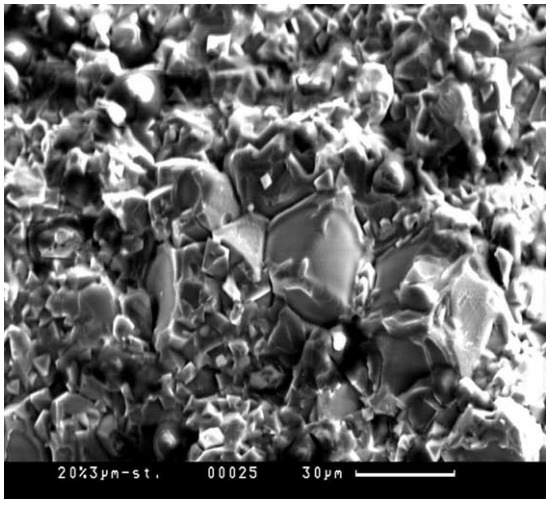

Fig. 12. Fracture surface of composite containing 20% 3 μm preformed spinel.

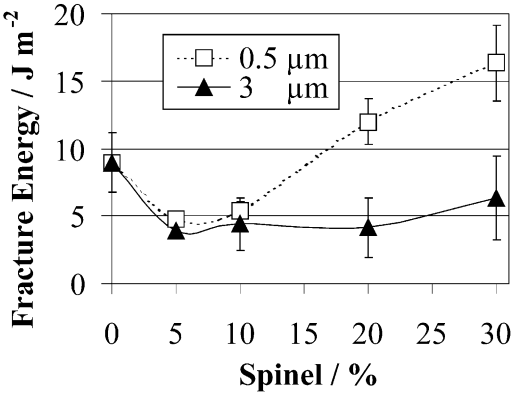

Fig. 13. Fracture surface energy as a function of in situ formed (0.5 μm) and preformed (3 μm) spinel content.

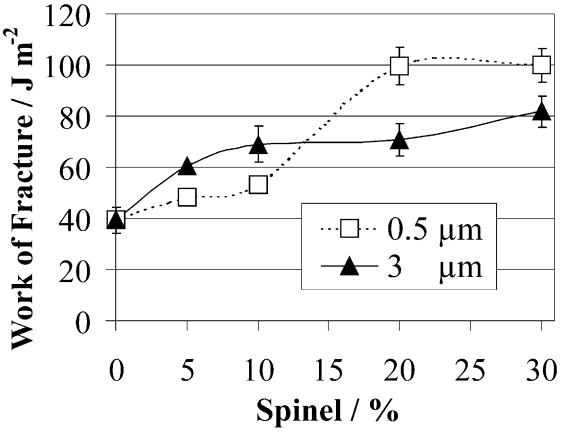

Fig. 14. Work of fracture as a function of in situ formed (0.5 μm) and preformed (3 μm) spinel content.

composition than Young's modulus; though the modulus values decreased with further additions of spinel, strengths remained approximately constant (Figs. 1 and 3). The thermal shock resistance of 20% 0.5 μm in situ formed spinel composites, in terms of the R'''' parameter, would therefore be predicted to be ~10% and ⩾4 times greater than that of both 3 μm preformed spinel composites and pure MgO, respectively. On the other hand, there was a sharp decline at 30% in the R'''' parameter values of in situ formed spinel composites, but R'''' reached the highest value by the addition of preformed 30% 3 μm spinel (Fig. 15). This increase in R'''' parameter appears mainly to be the result of the marked increase in γ_{WOF} with spinel additions (Fig. 14), and the greater sensitivity of strength to composition and particle size than Young's modulus (Figs. 1 and 3). This may be because the decline in strength with increasing spinel content is now very much greater than the corresponding decrease in Young's modulus, apart from increased γ_{WOF} values.

The observed changes in K_{1c}, γ_i and γ_{WOF} for these materials are in general accord with this predicted R'''' parameter, which showed similar patterns in terms of variations with spinel content (Fig. 15). It would be predicted on this basis that the in situ formed 20% 0.5 μm and 30% 3 μm preformed spinel composites would provide a significant improvement in resistance to thermal shock damage through increased difficulty of crack propagation in comparison with pure MgO. Furthermore, in the MgO–spinel composites a large amount of cracking is created during cooling, as a result of high tensile hoop stresses generated around the spinel particles, due to the large thermal expansion difference between MgO and spinel. The improved resistance predicted to thermal shock in these model MgO–spinel microcomposites can therefore be attributed to the microcrack networks developed around the spinel particles.

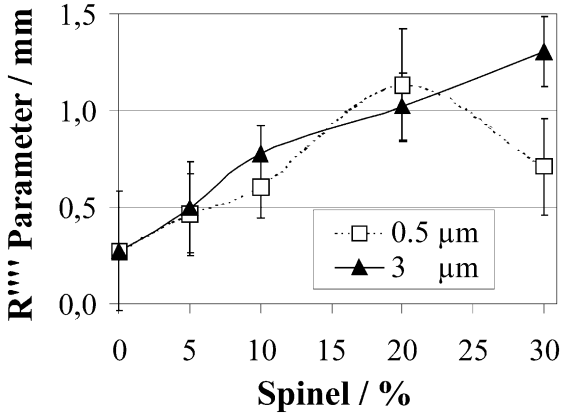

Fig. 15. R'''' parameter as a function of in situ formed (0.5 μm) and preformed (3 μm) spinel content.

4. Conclusions

The relationships between K_{1c} and fracture surface energy were similar to each other, and generally decreased with increasing preformed spinel content, apart from the in situ formed composites, which showed different microstructures and fracture paths. Fracture surfaces of MgO, and composites containing 5–10% spinel, showed mostly transgranular, with some intergranular, fracture. In contrast, spinel composites, containing ⩾20% spinel additions, primarily intergranular fracture occurred through the MgO grains, and it appears to require more energy to propagate a crack completely through the specimen. It is therefore clear that the development of thermal shock resistance in the in situ formed MgO–spinel composites can be linked to increased fracture toughness and work of fracture.

The improvement in thermal shock resistance predicted by the R'''' parameter, was explained by the large decreases in strength, and the lesser decreases in Young's modulus, with the high values of work of fracture. The in situ formed 20% 0.5 μm and 30% 3 μm preformed spinel composites showed the highest R'''' values, and it therefore would show greater resistance to crack propagation, and to further thermal shock damage, in comparison with pure MgO. To improve thermal shock resistance, there was no advantage with additions of ⩾30% in situ formed 0.5 μm spinel, as compared to 3 μm preformed spinel composites, for which a high amount of spinel content was required to achieve a comparable improvement.

Acknowledgements

The contributions of the late Professor R.W. Davidge and Professor B. Rand are gratefully acknowledged. P. Bartha, S. Plint, and M.W. Roberts are also thanked for helpful discussions. Alcoa International (UK) Ltd. is thanked for supplies of materials. Financial support was provided by the Council of Higher Education in Turkey.

References

1. Wilson, D. R., Evans, R. M., Wadsworth, I. and Cawley, J., Properties and applications of sintered magnesia alumina spinels. In *Proc. UNITECR '93 Congress*, Sao Paulo, Brazil, 1993, pp. 749–760.
2. Laurich-McIntyre, S. E. and Bradt, R. C., Room temperature strengths of individual tabular alumina and sintered spinel grains (aggregates). In *Proc. UNITECR '93 Congress*, Sao Paulo, Brazil, 1993, pp. 256–264.
3. Klischat, H. J. and Bartha, P., Further development of magnesia spinel bricks with their own specific properties for lining the transition and sintering zones of rotary cement kilns. *World Cement*, 1992, 52–58.

4. Reyes Sanchez, J. A. and Toledo, O. D., New developments of magnesite-chrome brick and magnesite-spinel for cement rotary kilns higher thermal shock resistance and higher coating adherence. In *Proc. UNITECR 89 Congress*, Anaheim, USA, 1989, pp. 968–979.
5. Sarkar, R., Das, S. K. and Banerjee, G., Effect of additives on the densification of reaction sintered and presynthesised spinels. *Ceram. Int*., 2003, **29**, 55–59.
6. Eusner, G. R. and Hubble, D. H., Technology of spinel-bonded periclase brick. *J. Am. Ceram. Soc*., 1960, **43**(6), 292–296.
7. Bartha, P., Magnesia spinel bricks—properties, production and use. In *Proc. Int. Symp. Refractories, Refractory Raw Materials and High Performance Refractory Products*, ed. X. Zhong *et al.* Pergamon, Hangzhou, 1989, pp. 661–674.
8. Sarkar, R., Das, S. K. and Banerjee, G., Effect of addition of Cr_2O_3 on the properties of MgO-Al_2O_3 spinels. *J. Eur. Ceram. Soc*., 2002, **22**, 1243–1250.
9. Moore, B., Frith, M. and Evans, D., Developments in basic refractories for cement kilns. *World Cement*, 1991, 5–12.
10. Dal Maschio, R., Fabbri, B. and Fiori, C., Industrial applications of refractories containing magnesium aluminate spinel. *Ind. Ceramics*, 1988, **8**(3), 121–126.
11. Gonsalves, G. E., Duarte, A. K. and Brant, P. O. R. C., Magnesia–spinel brick for cement rotary kilns. *Am. Ceram. Soc. Bull*., 1993, **72**(2), 49–54.
12. Evans, R. M., Magnesia-alumina spinel raw materials production and preparation. *Am. Ceram. Soc. Bull*., 1993, **72**(4), 59–63.
13. Steetley Magnesia Products Limited, Steetley Co., January 1993, 1–3.
14. Carbone, T. J., Characterization and refractory properties of magnesium aluminate spinel raw materials. *Interceram Spec. Issue*, 1985, 91–94.
15. Bartha, P., Using magnesia–spinel bricks to prevent the formation of rings in rotary cement kilns. *World Cement*, 1990, 98–100.
16. Jain, M. K. and Richter, T., Magnesia–alumina spinel refractories based on residue from a plasma dross recovery process. In *Proc. UNITECR '93 Congress*, Sao Paulo, Brazil, 1993, pp. 1039–1040.
17. *Modern Refractory Practice*. Harbison-Walker Refractories Company, Pittsburgh, Pennsylvania, 1961.
18. Soady, J. S. and Plint, S., A quantitative thermal shock approach to the development of magnesia–spinel refractories for the cement kiln. In *Proc. UNITECR '91 Congress*, Aachen, Germany, 1991, pp. 443–449.
19. Harburg, H. K. F., Experience with magnesium–aluminium–spinel bricks in a 3000 t/d rotary kiln. *Zement-Kalk-Gibs International*, 1993, **3/4**, 446–454.
20. Sarkar, R. and Banerjee, G., Magnesium aluminate spinel from single stage sintering. *Science of Sintering*, 2000, **32**, 61–68.
21. Roy, D. M., Roy, R. and Osborn, E. F., The system MgO-Al_2O_3-H_2O and the influence of carbonate and nitrate ions on the phase equilibria. *Am. J. Science*, 1953, **251**, 337–361.
22. Shackelford, J. F., Alexander, W., Park, J. S., eds., *CRC Materials Science and Engineering Handbook*. CRC Press, Boca Raton, Florida, 1994.
23. Burnett, S. J., *Properties of Refractory Materials*. UKAEA Research Group Report, Harwell, 1969.
24. Aksel, C., Rand, B., Riley, F. L. and Warren, P. D., Mechanical properties of magnesia–spinel composites. *J. Eur. Ceram. Soc*., 2002, **22**(5), 745–754.
25. Aksel, C. and Warren, P. D., Thermal shock parameters [R, R‴ and R⁗] of magnesia–spinel composites. *J. Eur. Ceram. Soc*., 2003, **23**(2), 301–308.
26. Aksel, C. and Warren, P. D., Work of fracture and fracture surface energy of magnesia–spinel composites. *Compos. Sci. Technol*, 2003, **63**(10), 1433–1440.
27. Tabbert, W. and Klischat, H. J., Magnesia spinel bricks for the cement industry. In *Proceedings Beijing China Symposium*, China, 1992, pp. 424–430.
28. Aksel, C., Davidge, R. W., Warren, P. D. and Riley, F. L., Investigation of thermal shock resistance in model magnesia–spinel refractory materials. In *IV. Ceramic Congress*, Proceedings Book, Part 1, Eskisehir, Turkey, 1998, pp. 193–199.
29. Davidge, R. W., *Mechanical Behaviour of Ceramics*. Cambridge University Press, Cambridge, 1979.
30. Mastelaro, R. V. and Zanotto, E. D., Residual stresses in a soda-lime-silica glass-ceramic. *J. Non-Cryst. Solids*, 1996, **194**, 297–304.
31. Aksel, C., Davidge, R. W., Warren, P. D. and Riley, F. L., Mechanical properties of model magnesia-spinel composite materials. Euro Ceramics V, Part 3, Extended Abstracts of the 5th Conference and Exhibition of the European Ceramic Society, In *Key Engineering Materials*, vols. 132–136, Versailles, France, 1997, pp. 1774–1777.
32. Aksel, C., Davidge, R. W., Knott, P. and Riley, F. L., Mechanical properties of magnesia-magnesium aluminate spinel composites. In *III. Ceramic Congress Proceedings Book*, Engineering Ceramics, vol. 2, Istanbul, Turkey, 1996, pp. 172–179.
33. Aksel, C. *Thermal Shock Behaviour and Mechanical Properties of Magnesia–Spinel Composites*. PhD Thesis, Department of Materials Engineering, University of Leeds, Leeds, UK, 1998.
34. Aksel, C., Warren, P. D. and Riley, F. L., Fracture behaviour of magnesia and magnesia–spinel composites before and after thermal shock. *J. Eur. Ceram. Soc*., 2004, **24**(8), 2407–2416.
35. Aksel, C., Rand, B., Riley, F. L. and Warren, P. D., Thermal shock behaviour of magnesia–spinel composites. *J. Eur. Ceram. Soc*., 2004, **24**(9), 2839–2845.
36. Kimura, M., Yasuda, Y. and Nishio, H., Development of magnesia spinel bricks for rotary cement kilns in Japan. In *Proc. 26th Int. Col. Ref*., vol. 33, Interceram Special Issue, Aachen, Germany, 1984, pp. 344–376.
37. Hasselman, D. P. H., Elastic energy at fracture and surface energy as design criteria for thermal shock. *J. Am. Ceram. Soc*., 1963, **46**, 535–540.
38. Hasselman, D. P. H., Unified theory of thermal shock fracture initiation and crack propagation in brittle ceramics. *J. Am. Ceram. Soc*., 1969, **52**, 600–604.
39. Chaklader, A. C. D., and Bradley, F., Thermal shock resistance parameters and their application to refractories. In *Proc. UNITECR '89 Congress*, Anaheim, USA, 1989, pp. 1225–1236.
40. Aksel, C. and Riley, F. L., Effect of particle size distribution of spinel on the mechanical properties and thermal shock performance of MgO–spinel composites. *J. Eur. Ceram. Soc*., 2003, **23**(16), 3079–3087.
41. *BS 7134, Methods for Determination of Density and Porosity*. British Standard Testing of Engineering Ceramics, Part 1, Section 1.2, 1989.
42. ASTM C1161-90, *Standard Test Method for Flexural Strength of Advanced Ceramics at Ambient Temperature*, vol. 15.01. Annual Book of ASTM Standards, ASTM, 1991.
43. ASTM D790M-86, *Standard Test Methods for Flexural Properties of Unreinforced and Reinforced Plastics and Electrical Insulating Materials*, vol. 08.01. Annual book of ASTM Standards, ASTM, 1988.
44. Larson, D. R., Coppola, J. A., Hasselman, D. P. H. and Bradt, R. C., Fracture toughness and spalling behaviour of high-Al_2O_3 refractories. *J. Am. Ceram. Soc*., 1974, **57**, 417–421.
45. ASTM E399-90, *Standard Test Method for Plane-Strain Fracture Toughness of Metallic Materials*, vol. 03.01, Annual Book of ASTM Standards, ASTM, 1991.
46. ASTM D5045-91, *Standard Test Methods for Plane-Strain Fracture Toughness and Strain Energy Release Rate of Plastic Materials*, vol. 08.03. Annual Book of ASTM Standards, ASTM, 1991.
47. Brown, W. F. and Srawley, J. E., *Plane Strain Crack Toughness Testing of High Strength Metallic Materials*. ASTM Special Technical Publication, No: 410. 1967.

48. Davidge, R. W. and Tappin, G., The effective surface energy of brittle materials. *J. Mater. Sci.*, 1967, **3**, 165–173.
49. Coppola, J. A., Hasselman, D. P. H. and Bradt, R. C., On the measurement of the work-of-fracture of refractories. *Am. Ceram. Soc. Bull.*, 1972, **17**, 578.
50. Mendelson, M. I., Average grain size in polycrystalline ceramics. *J. Am. Ceram. Soc.*, 1969, **52**, 443–446.
51. Rice, R. W., Strength and fracture of hot-pressed MgO. *Proc. Brit. Ceram. Soc.*, 1972, **20**, 329–363.
52. Aksel, C. and Riley, F. L., Young's modulus measurements of magnesia–spinel composites using load–deflection curves, sonic modulus, strain gauges and Rayleigh waves. *J. Eur. Ceram. Soc.*, 2003, **23**(16), 3089–3096.
53. Llorca, J. and Ogawa, T., In: ed. R. C., Bradt, D. P. H., Hasselman, D., Munz, M., Sakai, and V. Ya., Shevchenko, Crack wake effects on MgO fracture resistance. In *Fracture Mechanics of Ceramics*, vol. 9. 1992, pp. 305–317.
54. Evans, A. G., Energies for crack propagation in polycrystalline MgO. *Philos. Mag*, 1970, **22**, 841–852.
55. Davidge, R. W., The texture of special ceramics with particular reference to mechanical properties. *Proc. Brit. Ceram. Soc.*, 1972, **20**, 364–378.
56. Uchno, J. J., Bradt, R. C. and Hasselman, D. P. H., Fracture surface energies of magnesite refractories. *Am. Ceram. Soc. Bull.*, 1976, **55**, 665–668.
57. Stewart, R. L. and Bradt, R. C., Fracture of polycrystalline $MgAl_2O_4$. *J. Am. Ceram. Soc.*, 1980, **63**, 619–623.
58. Stewart, R. L. and Bradt, R. C., Fracture of single crystal $MgAl_2O_4$. *J. Mater. Sci.*, 1980, **15**, 67–72.
59. Swanson, G. D., Fracture energies of ceramics. *J. Am. Ceram. Soc.*, 1972, **55**, 48–49.
60. Clarke, F. J. P., Tattersall, H. G. and Tappin, G., Toughness of ceramics and their work of fracture. *Proc. Brit. Ceram. Soc.*, 1966, **6**, 163–172.